

# Trap and population imbalanced two-component Fermi gas in the BEC limit

S. A. Silotri\*

*Theoretical Physics Division, Physical Research Laboratory, Ahmedabad 380009, India*

(Dated: November 20, 2018)

We study equal mass population imbalanced two-component atomic Fermi gas with unequal trap frequencies ( $\omega_\uparrow \neq \omega_\downarrow$ ) at zero temperature using the local density approximation (LDA). We consider the strongly attracting Bose-Einstein condensation (BEC) limit where polarized (gapless) superfluid is stable. The system exhibits shell structure: unpolarized SF  $\rightarrow$  polarized SF  $\rightarrow$  normal N. Compared to trap symmetric case, when the majority component is tightly confined the gapless superfluid shell grows in size leading to reduced threshold polarization to form polarized (gapless) superfluid core. In contrast, when the minority component is tightly confined, we find that the superfluid phase is dominated by unpolarized superfluid phase with gapless phase forming a narrow shell. The shell radii for various phases as a function of polarization at different values of trap asymmetry are presented and the features are explained using the phase diagram.

PACS numbers: 03.75.Ss, 03.75.Hh, 67.85.Lm

## INTRODUCTION

Ultracold atomic Fermi gases present a unique opportunity to study the exotic pairing phases where the effective interaction is tunable via Feshbach resonance and population of each spin component can be controlled. These studies with two-component Fermi gas include the Bardeen-Cooper-Schrieffer (BCS) to Bose-Einstein condensation (BEC) crossover [1, 2] with equal population two-component Fermi gas and the effects of population imbalance on the superfluid state [2, 3, 4, 5, 6, 7, 8, 9]. For Fermi gas with population imbalance, various pairing scenarios are proposed: Fulde-Ferrel-Larkin-Ovchinnikov phase FFLO [10, 11], breached pairing [12], phase separation [13] and pairing with deformed fermi surface [14].

The present studies of equal mass superfluid Fermi systems involve same trapping potentials for the two component. The zero [15] and finite temperature [16] phase diagrams of the equal mass population imbalanced system taking into account various pairing phases with implications to experiments are well understood. The trap imbalanced is naturally realized with Fermi mixture with unequal masses where each component experiences different potential due to the mass difference. The ground state properties for this system have been studied in Ref. [17, 18, 19, 20]. However, it was recently proposed in Ref. [25] that even equal mass Fermi mixture can admit trap imbalance and the system was studied with population balance [25] and small trap imbalance [26].

Motivated by recent experiment performed in the BEC regime of interaction exploring Bose-Fermi mixture [9], we consider the trap and population imbalanced ( $\omega_\uparrow \neq \omega_\downarrow$ ) Fermi mixture in this regime. The phase diagram in this regime becomes richer with the existence of the gapless (polarized) superfluid also referred to as breached pair phase with one fermi surface. We study the effects of trap asymmetry on the shell structure as function of polarization. The shell structure, in general, consists of

three phases: unpolarized superfluid (BCS SF) at the center, the breached pair phase with one fermi surface (BP1) forms the intermediate shell finally surrounded by polarized normal (N). We do not consider the FFLO phase [10, 11] where cooper pair carries finite center-of-mass momentum. This phase is stable within very narrow window of the applied chemical potential difference in the BCS regime.

## FORMALISM

The system we consider is a trapped cloud of two-component Fermionic mixture confined by harmonic isotropic potential  $V_{T\sigma}(r)$  where  $r$  measures the distance from the trap center. The Fermi atoms have unequal population of the two pseudo-spin (hyperfine) states and interact via point-contact  $s$ -wave interaction. To proceed further we start with system without the trap and later include it under local density approximation. The Hamiltonian density ( $\hbar = 1$ ) for the fermions in this case is given by

$$H = \sum_{\sigma} \Psi_{\sigma}^{\dagger}(\mathbf{r}) (\varepsilon_{k\sigma} - \mu_{\sigma}) \Psi_{\sigma}(\mathbf{r}) + g \Psi_{\uparrow}^{\dagger}(\mathbf{r}) \Psi_{\downarrow}^{\dagger}(\mathbf{r}) \Psi_{\downarrow}(\mathbf{r}) \Psi_{\uparrow}(\mathbf{r}), \quad (1)$$

where  $\Psi_{\sigma}^{\dagger}(\mathbf{r})$  creates a pseudospin- $\sigma$  fermion at position  $\mathbf{r}$ ,  $\varepsilon_{k\sigma} = k^2/2m_{\sigma}$ ;  $\mu_{\sigma}$  and  $m_{\sigma}$  are the chemical potential and mass for pseudospin- $\sigma$  component with  $\sigma = \uparrow, \downarrow$ .  $g$  is the bare coupling constant characterizing interparticle interaction. It is related to  $s$ -wave scattering length  $a$  of the system by the Lippmann-Schwinger equation

$$\frac{\tilde{m}}{2\pi a} = \frac{1}{g} + \frac{1}{V} \sum_{\mathbf{k}} \frac{1}{2\varepsilon_{\mathbf{k}}}, \quad (2)$$

where the average kinetic energy  $\varepsilon_{\mathbf{k}} = (\varepsilon_{1\mathbf{k}} + \varepsilon_{2\mathbf{k}})/2$ ,  $V$  is volume and reduced mass  $\tilde{m} = m_{\uparrow}m_{\downarrow}/(m_{\uparrow} + m_{\downarrow})$ . The pairing Hamiltonian can be diagonalized by Bogoliubov

transformations using thermofield dynamics techniques as described in [21, 22]. This formalism also accounts for the polarized superfluidity when two components have unequal population or masses. This leads to thermodynamic potential density,

$$\Omega = \frac{1}{V} \sum_{\mathbf{k}} \left[ \xi_{\mathbf{k}} - E_{\mathbf{k}} - \frac{1}{\beta} \sum_{\sigma} \ln(1 + \exp(-\beta E_{\sigma})) \right] - \frac{\Delta^2}{g}, \quad (3)$$

where we have defined gap or order parameter  $\Delta(\mathbf{r}) = -g \langle \Psi_{\downarrow}(\mathbf{r}) \Psi_{\uparrow}(\mathbf{r}) \rangle$ . Introducing the chemical potential  $\mu = (\mu_{\uparrow} + \mu_{\downarrow})/2$  and the chemical potential difference or the Zeeman field  $h = (\mu_{\uparrow} - \mu_{\downarrow})/2$ , we define quasiparticle energies  $E_{\sigma} = E \pm \delta\xi$  with  $\xi_{\mathbf{k}} = \varepsilon_{\mathbf{k}} - \mu$ ,  $E_{\mathbf{k}} = \sqrt{\xi_{\mathbf{k}}^2 + \Delta^2}$ , for equal mass case  $\delta\xi = -h$  and  $\beta = 1/T$ .

Note that there are two branches for the quasiparticle energies and lead to gapless modes when  $E_{k\uparrow} = 0$  assuming  $\uparrow$ -fermions to be majority. At zero temperature the excess fermions are accommodated in negative quasiparticle energy states. This gapless phase is referred to as breached pair phase with one Fermi surface (BP1) as it is stable only for  $\mu < 0$  and hence possesses one Fermi surface. In the deep BEC regime this phase can be understood as mixture of composite bosons and fermion quasiparticles [16].

The gap equation is given by the condition of extremum of thermodynamic potential density  $\frac{\partial \Omega}{\partial \Delta} = 0$ . The average number density and density difference equation respectively are given by  $n = -\frac{\partial \Omega}{\partial \mu}$  and  $m = -\frac{\partial \Omega}{\partial h}$ .

Before considering the trapped system, we construct the zero temperature phase diagram in grand canonical ensemble [24] of fixed  $\mu$  and  $h$ .

We start with  $h = 0$  and find the point where superfluid state make continuous transition to vacuum state of molecules. This value of  $\mu$  is denoted by  $\mu_c$ . For small  $h < h_m$  this behavior i.e. superfluid-to-Vacuum persists and leads to vertical phase boundary in the diagram.

Next, we start with  $\mu < \mu_c$  and increasing  $h$ . Here system evolve from vacuum state to polarized normal state as  $\mu_{\uparrow} = \mu + h$  is now positive quantity leading to finite population of the  $\uparrow$ -fermions. There cannot be superfluid phase here as  $\mu < \mu_c$ . This leads to Vacuum-to-Polarized N phase boundary.

Similarly we start with  $\mu > \mu_c$  with increasing  $h$ . Here system makes continuous transition to Breached pair state as superfluid starts to admit finite polarization. The superfluid-to BP1 boundary is calculated by numerical comparison of the thermodynamic potential in the respective states. As we further increase the  $h$ , the BP1 eventually make transition to polarized normal state. However, depending on the value of  $\mu$  the BP1-to-Polarized transition can be first or second order. The tricritical point where first and second order transition meet is indicated in the phase diagram. Also the BP1-Normal first order curve intersect the superfluid-BP1 curve at

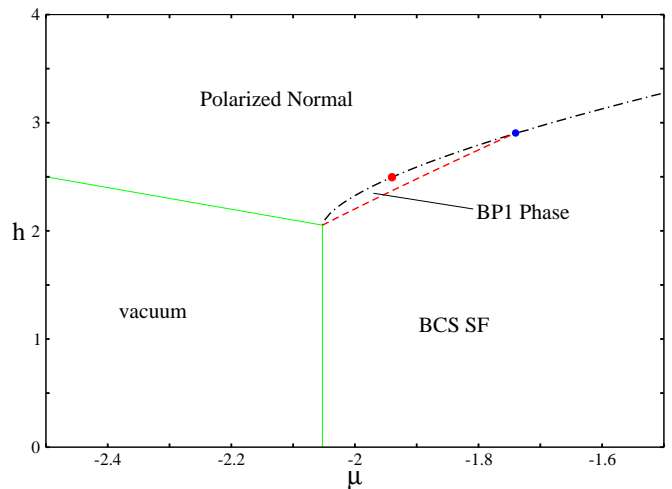


FIG. 1: (Color online) The zero temperature phase diagram for  $(k_F a)^{-1} = 2.0$  showing unpolarized superfluid (BCS SF), polarized superfluid (BP1), vacuum and polarized normal (N) phases. The upper (blue) dot denotes the point beyond which BP1 state ceases to exist. The lower (red) dot represents the tricritical point. The dashed (red) line indicates the second-order transition between unpolarized SF and BP1 phase. The dot dashed (black) line indicates first-order transition between SF to polarized N state and BP1 to normal above and below the upper (blue) point respectively.

large  $\mu$ . Beyond this intersection point, BP1 ceases to exist and there is direct first order superfluid-to-Normal transition.

## TRAPPED FERMION MIXTURE

We next consider the trapped fermions confined by harmonic isotropic potential. This can be taken into account via local density approximation (LDA) where trapped system is treated as locally uniform with local chemical potential  $\mu_{\sigma}(r) = \mu_{\sigma} - V_{T\sigma}$ .  $\mu_{\sigma}$  is actual Lagrange multiplier constraining number of atoms and  $V_{T\sigma} = \frac{1}{2} m_{\sigma} \Omega_{\sigma} r^2$  with  $\omega_{\sigma}$  as trapping frequency for component  $\sigma$ . Furthermore, the chemical potentials of each component at a given point in the trap can be written as

$$\mu_1(r) = \mu(r) + h(r) \quad (4)$$

$$\mu_2(r) = \mu(r) - h(r) \quad (5)$$

where  $\mu(r) = \mu - V_T(r)$  and  $h(r) = h - \delta V_T(r)$  where  $V_T(r) = (V_{T\uparrow} + V_{T\downarrow})/2$  and  $\delta V_T(r) = (V_{T\uparrow} - V_{T\downarrow})/2$ . The quantities  $\mu$  and  $h$  are determined by enforcing particle number constraints namely total number of atoms and population difference respectively.

In terms of  $n(r) = n_{\uparrow}(r) + n_{\downarrow}(r)$  and  $m(r) = n_{\uparrow}(r) - n_{\downarrow}(r)$ , the total number of atoms  $N$  and population imbalance  $\Delta N$  are given by  $N = \int d^3r n(r)$  and  $\Delta N =$

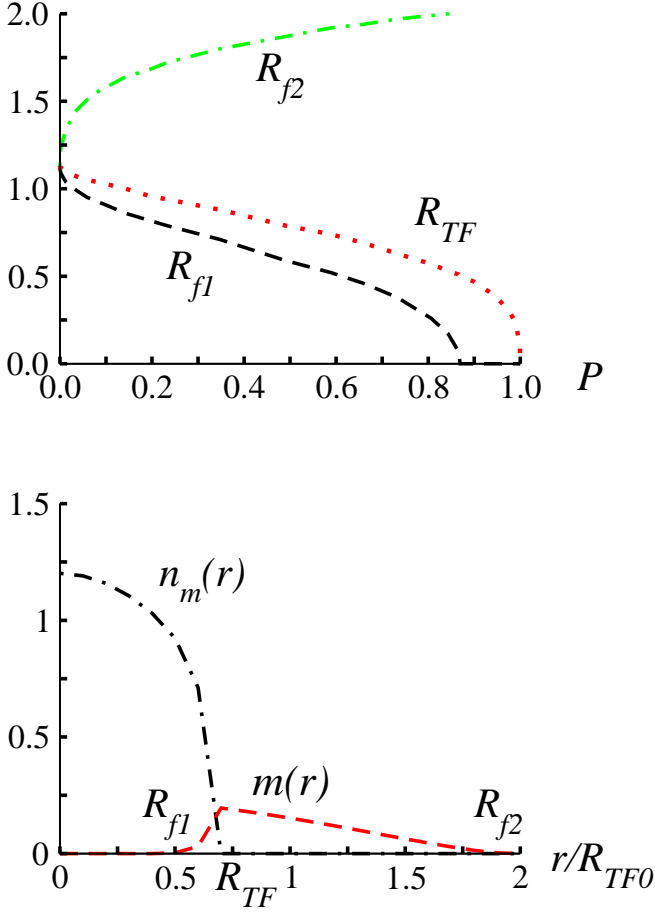


FIG. 2: (Color online) (a) The three radii  $R_{f1}$  (outer boundary of unpolarized superfluid),  $R_{TF}$  (outer boundary of BP-1 phase) and  $R_{f2}$  (outer boundary of N phase) plotted as a function of polarization  $P$  at trap asymmetry parameter  $\eta = 0$  and  $(k_F a)^{-1} = 2.0$ . (b) The molecular density  $n_m$  and magnetization  $m$  plotted against radius  $r$  measured in units of  $k_F^3$  and  $R_{TF0}$ .

$\int d^3r m(r)$  where

$$n_{\uparrow}(r) = \frac{1}{(2\pi)^3} \int d^3k \left[ \frac{1}{2} \left( 1 + \frac{\xi(r)}{E(r)} \right) \Theta(-E_{\uparrow}(r)) + \frac{1}{2} \left( 1 - \frac{\xi(r)}{E(r)} \right) (1 - \Theta(-E_{\downarrow}(r))) \right] \quad (6)$$

$$n_{\downarrow}(r) = \frac{1}{(2\pi)^3} \int d^3k \left[ \frac{1}{2} \left( 1 + \frac{\xi(r)}{E(r)} \right) \Theta(-E_{\downarrow}(r)) + \frac{1}{2} \left( 1 - \frac{\xi(r)}{E(r)} \right) (1 - \Theta(-E_{\uparrow}(r))) \right]. \quad (7)$$

where  $\Theta(\dots)$  is the Heaviside step function, the zero-temperature limit for Fermi-Dirac distribution. The local gap equation is

$$-\frac{\tilde{m}}{2\pi a} = \frac{1}{(2\pi)^3} \int d^3k \left[ \frac{1}{2E(r)} (1 - \Theta(-E_{\uparrow}(r)) - \Theta(-E_{\downarrow}(r))) - \frac{1}{2\varepsilon_k} \right]. \quad (8)$$

The trap introduces the new length scale called Thomas-Fermi radius defined as  $R_{TF} = \sqrt{\frac{2\mu}{m\omega_T^2}}$ . Note further that in the BEC regime, chemical potential  $\mu$  is already negative at the center of the trap and hence  $\mu(r)$  does not vanish. We also note that in the deep BEC regime  $\mu = -E_b/2$  [23], the molecular binding energy with  $E_b = 1/2m_r a^2$ . Thus we impose the condition [24],

$$\mu(R_{TF}0) = \mu_0 - \frac{1}{2}m\omega_T^2 R_{TF0}^2 = -\frac{E_b}{2}. \quad (9)$$

This gives,

$$R_{TF0} = \sqrt{\frac{E_b(2\mu_0 + 1)}{m\Omega_T^2}}. \quad (10)$$

The zero subscript indicates that the quantities are for zero polarization. To investigate the system numerically we define the dimensionless quantities  $\hat{\Delta}(r) = \Delta/E_F$ ,  $\hat{\mu}(r) = \mu(r)/E_F$ ,  $\hat{h}(r) = h(r)/E_F$  where we choose  $E_F = (6N)^{1/3}\hbar\Omega_T$  with  $\omega_T = \sqrt{\omega_{\uparrow}^2 + \omega_{\downarrow}^2}$ . We, also, normalize the distance in the trap  $x = r/R_{TF0}$  and define  $k_F$  by the relation  $E_F = k_F^2/2\tilde{m}$ . Hence

$$\hat{\mu}_0(x) = \hat{\mu}_0 - x^2 \left( \hat{\mu}_0 + \frac{1}{(k_F a)^2} \right), \quad (11)$$

where we have expressed the binding energy  $E_b$  in  $E_F$  units as  $E_b = E_F/(k_F a)^2$ . However for the system with population imbalance we have

$$\hat{\mu}(x) = \hat{\mu} - \left( \hat{\mu}_0 + \frac{1}{(k_F a)^2} \right) x^2, \quad (12)$$

$$\hat{h}(x) = \hat{h} - \eta \left( \hat{\mu}_0 + \frac{1}{(k_F a)^2} \right) x^2,$$

where dimensionless quantity  $\eta = (\omega_{\uparrow}^2 - \omega_{\downarrow}^2)/(\omega_{\uparrow}^2 + \omega_{\downarrow}^2)$  controls the trap asymmetry of the Fermi gas.

Now the equation for total number of atoms and population difference in dimensionless form are given by

$$N = \int d^3x n(\hat{\mu}(x), \hat{h}(x)), \quad (13)$$

$$\Delta N = \int d^3x m(\hat{\mu}(x), \hat{h}(x)). \quad (14)$$

The system for a given coupling strength and polarization  $P = \Delta N/N$  is investigated numerically in the following manner: first  $\mu_0$  is calculated by setting  $P = 0$ . Then using Eq. 12 together with number and population imbalance equation,  $\mu$  and  $h$  are calculated. In the BEC limit the order parameter ( $\Delta$ ) and density for composite bosons or molecular density are related [23]. By calculating the local composite boson density ( $n_m$ ) and magnetization ( $m$ ), the various phases are identified.

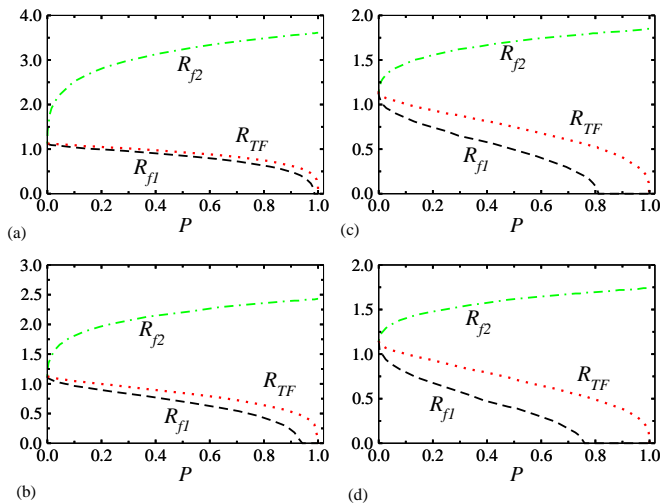


FIG. 3: (Color online) The three radii  $R_{f1}$  (outer boundary of unpolarized superfluid),  $R_{TF}$  (outer boundary of BP1 phase) and  $R_{f2}$  (outer boundary of N phase) plotted as a function of polarization  $P$  for various values of the trap asymmetry parameter  $\eta$ . (a)  $\eta = -0.9$ , (b)  $\eta = -0.5$  (c)  $\eta = 0.5$ , (d)  $\eta = 0.9$ . All the radii are measured in units of  $R_{TF0}$  (outer boundary of superfluid unpolarized cloud).

## RESULTS AND DISCUSSIONS

We choose experimentally accessible  $(k_F a)^{-1} = 2.0$  for the interaction strength. The phase at each spatial point of the trap is determined by the local chemical potentials  $\mu(r)$  and  $h(r)$  (see Eqs. 12) mapping it to the corresponding point in the phase diagram. As radius is increased ( $\mu(r), h(r)$ ) moves towards left in the phase diagram forming a line segment.

We find three different phases in the cloud. At the center, superfluid core where the population of the two components are equal i.e. unpolarized superfluid (BCS SF), then an intermediate polarized superfluid (BP1) shell where fermion quasiparticles and composite bosons coexist and finally outer rim of majority component. This leads to three radii characterizing the shell structure:  $R_{f1}$  where  $n_m \neq 0$  and  $m(r) = 0$  forming boundary for BCS SF phase,  $R_{TF}$  above which  $n_m = 0$  and  $R_{f2}$  above which  $m(r) = 0$ .

The three radii for the system without trap asymmetry  $\eta = 0$  as a function of polarization  $P$  together with density profiles showing  $n_m(r)$  and  $m(r)$  are shown in Fig. 2. The shell structure consist of BCS SF phase for  $r < R_{f1}$ , BP1 phase for  $R_{f1} < r < R_{TF}$ . and finally polarized normal (N) state for  $R_{TF} < r < R_{f2}$ .

We next consider the system with trap asymmetry characterized by the dimensionless parameter  $\eta = (\omega_{\uparrow}^2 - \omega_{\downarrow}^2)/(\omega_{\uparrow}^2 + \omega_{\downarrow}^2)$ . The positive (negative)  $\eta$  value indicates that majority (minority) component is more tightly confined harmonically than the minority (majority) component.

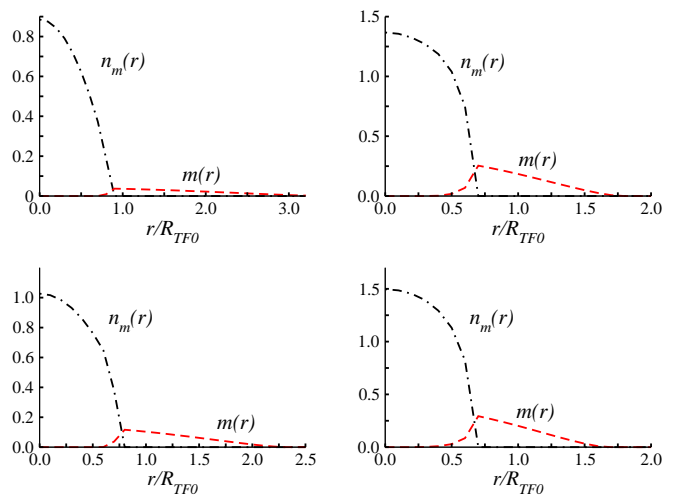


FIG. 4: (Color online) Density profiles at  $P = 0.65$  for different values of the trap asymmetry parameter  $\eta$ . (a)  $\eta = -0.9$ , (b)  $\eta = -0.5$  (c)  $\eta = 0.5$ , (d)  $\eta = 0.9$ . The molecular density  $n_m$  and the magnetization plotted as a function of radius measured in units of  $k_F^3$  and  $R_{TF0}$  respectively.

The three radii with different trap asymmetry parameter  $\eta$  as functions of polarization  $P$  are shown in Fig. 3. The value  $\eta \pm 0.9$  corresponds to the situation when one of the component is very strongly confined. We start with  $\eta = -0.9$  corresponding to  $\omega_{\uparrow} \ll \omega_{\downarrow}$ . The BP1 shell here is very narrow and overall size of the cloud (characterized by  $R_{f2}$ ) is much larger than the superfluid cloud without population imbalance (the cloud size is measured in units of  $R_{TF0}$ ). As we increase  $\eta$ , the BP1 shell grows in size, however, size of the cloud decreases. The window of polarization for which BP1 phase forms the superfluid core starting at the center of the trap increases becoming maximum at  $\eta = 0.9$ . The BP1 phase forms the core beginning at  $P = 0.76$ , which should be experimentally feasible. We also present the density profiles for same set of  $\eta$  at  $P = 0.65$  in Fig. 4. We note that as  $\eta$  increases, size of  $n_m$  representing density of the composite bosons shrinks but becomes more dense. It also exhibits the large cloud sizes for tightly confined minority as noted above.

All these features can be explained by analyzing  $(\mu(r), h(r))$  variations for each value of  $\eta$  in the phase diagram. To this end, we replot the phase diagram enlarging the BP1 state. The line segments representing above mentioned variations are also shown (Fig. 5). We note that  $\eta$  with positive (negative) value has a positive (negative) slopes with zero value for  $\eta = 0$ .

Note further that BP1 to polarized N transition is second and first order for positive and negative set of chosen values respectively. These transitions can be detected via density profiles in the experiments.

The  $\eta = -0.9$  line segment traverses small region of BP1 phase making second order transition to polarized

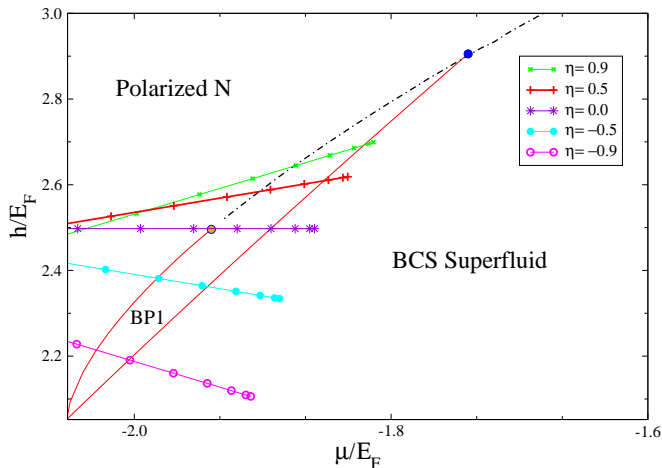


FIG. 5: (Color online) The part of phase diagram with the BP-1 region enlarged. The solid (red) line indicates the second order phase transition and dot dashed (black) line shows first order transition. Superimposed are the  $\mu - h$  variations as line segments for various values of the trap asymmetry parameter  $\eta$  at  $P = 0.65$

N while  $\eta = 0.9$  segment traverses larger region in BP-1 phase before making first order transition to polarized N. The order of transition can be detected in experiments via spatial discontinuities which vanish for second order transition. As  $\eta$  is increased from  $\eta = -0.9$  line segment increasingly have larger portion in BP-1 region. This explains why the BP1 shell expands in size as  $\eta$  is increased. Note further that owing to their negative (positive) slopes,  $\eta$  with negative values have longer (shorter) excursion into the polarized N state before encountering the vacuum explaining the larger (smaller) size for their clouds. Since all the atoms are integrated across the trap to conserve the atoms, the corresponding atom density distributions are also affected accounting for increased (reduced) number of atoms in BP1 phase for  $\omega_{\uparrow} > \omega_{\downarrow}$  ( $\omega_{\uparrow} < \omega_{\downarrow}$ ).

## CONCLUSION

In conclusion, we have studied in this paper the asymmetrically trapped and population imbalanced two-components Fermi gas in the strongly attracting BEC limit at  $T = 0$ . Using the local density approximation (LDA), we calculated the shell radii of various phases in the trap as a function of polarization and trap asymmetry. Compared to symmetric trap case ( $\eta = 0$ ), we find that when the majority component is tightly confined the gapless superfluid shell (BP1) increases in size. The polarization threshold to form the polarized BP1 superfluid at the core is reduced for a given interaction strength in this case. However, when minority are tightly confined

unpolarized superfluid is favored with BP1 phase forming a narrow shell. We explained these features using the phase diagram.

We wish to thank H. Mishra and D. Angom for discussions at the initial stages of this work.

\* Electronic address: silotri@prl.res.in

- [1] See, *e.g.*, S. Giorgini, L.P. Pitaevskii and S. Stringari, Rev. Mod. Phys. **80**, 1215 (2008) and references therein.
- [2] W. Ketterle, Y. Shin, A. Schirotzek and C. H. Shunk J. Phys.: condens. Matter **21**, 164206 (2009).
- [3] M.W. Zwierlein, A. Schirotzek, C.H. Schunck and W. Ketterle, Science **311**, 492 (2006).
- [4] G.B. Partridge, W. Li, R.I. Kamar, Y.A. Liao and R.G. Hulet, Science **311**, 503 (2006).
- [5] M.W. Zwierlein, C.H. Schunck, A. Schirotzek, W. Ketterle, Nature **442**, 54 (2006).
- [6] Y. Shin, M.W. Zwierlein, C.H. Schunck, A. Schirotzek and W. Ketterle, Phys. Rev. Lett. **97**, 030401 (2006).
- [7] C. H. Schunck, Y. Shin, A. Schirotzek, M. W. Zwierlein, and W. Ketterle, Science **316**, 867 (2007).
- [8] Y. Shin, C.H. Schunck, A. Schirotzek and W. Ketterle, Nature **451**, 689 (2008).
- [9] Y. Shin, A. Schirotzek, C.H. Schunck, and W. Ketterle Phys. Rev. Lett. **101**, 070404 (2008).
- [10] P. Fulde and R. A. Ferrell, Phys. Rev. **135**, A550 (1964).
- [11] A. I. Larkin and Y. N. Ovchinnikov, Sov. Phys. JETP **20**, 762 (1965).
- [12] W. V. Liu and F. Wilczek, Phys. Rev. Lett. **90**, 047002 (2003).
- [13] P. F. Bedaque, H. Caldas, and G. Rupak, Phys. Rev. Lett. **91**, 247002 (2003).
- [14] A. Sedrakian, J. Mur-Petit, A. Polls, and H. Muther, Phys. Rev. A **72**, 013613 (2005).
- [15] D. E. Sheehy and L. Radzihovsky, Phys. Rev. Lett. **96**, 060401 (2006).
- [16] M. M. Parish F. M. Marchetti, A. Lamacraft and B. D. Simons, Nature Phys. **3**, 124 (2007).
- [17] G. D Lin, W. Yi and L. M. Duan, Phys. Rev. A **74**, 031604(R) (2006).
- [18] M. Iskin C. A. R. Sá de Melo, Phys. Rev. Lett. **97**, 100404 (2006).
- [19] M. M. Parish, F. M. Marchetti, A. Lamacraft and B. D. Simons, Phys. Rev. Lett. **98**, 160402 (2007).
- [20] C. H. Pao, S. T. Wu and S. K. Yip, Phys. Rev. A **76**, 053621 (2007).
- [21] S. Silotri, D. Angom, H. Mishra and A. Mishra, Eur. Phys. Jr. D **49**, 383-390 (2008).
- [22] H. Mishra and A. Mishra, Eur. Phys. Jr. D **53**, 75-87, (2009).
- [23] C. A. R. Sá de Melo, M. Randeria, and J. R. Engelbrecht, Phys. Rev. Lett. **71**, 3202 (1993).
- [24] D. E. Sheehy and L. Radzihovsky, Annals of Physics **322**, 1790 (2007)
- [25] M. Iskin and C. J. Williams, Phys. Rev. A **77**, 013605, (2008).
- [26] D. Blume, Phys. Rev. A **78**, 013613, (2008).